EFFICIENT SILICON NITRIDE SiNx:H ANTIREFLECTIVE AND PASSIVATION LAYERS DEPOSITED BY ATMOSPHERIC PRESSURE PECVD FOR LOW COST PERC SOLAR CELLS

Jean-françois Lelièvre, Bishal Kafle, Pierre Saint-Cast, Paul Brunet, Romain Magnan, Emmanuel Hernandez, Sylvain Pouliquen, Françoise Massines

EFFICIENT SILICON NITRIDE SiN_x:H ANTIREFLECTIVE AND PASSIVATION LAYERS DEPOSITED BY ATMOSPHERIC PRESSURE PECVD FOR LOW COST PERC SOLAR CELLS

Jean-François Lelièvre[1,+], Bishal Kafle[2], Pierre Saint-Cast[2], Paul Brunet[1], Romain Magnan[1], Emmanuel Hernandez[1], Sylvain Pouliquen[3], Françoise Massines[1,*]

[1] *PROMES CNRS, UPR 8521, Tecnosud, Rambla de la thermodynamique, 66100 Perpignan, France*
jeanfrancois.lelievre@cea.fr; paul.brunet@promes.cnrs.fr ; romain.magnan@promes.cnrs.fr ; hernande@univ-perp.fr; francoise.massines@promes.cnrs.fr

[2] *Fraunhofer Institute for Solar Energy Systems, Heidenhofstrasse 2, 79110 Freiburg, Germany*
bishal.kafle@ise.fraunhofer.de ; pierre.saint-cast@ise.fraunhofer.de

[3] *Air Liquide, Paris-Saclay Research Center, 1 chemin du bas de la porte des Loges, 78350, Jouy en Josas, France*
sylvain.pouliquen@airliquide.com

[*] *Corresponding author: Françoise Massines;*
PROMES CNRS, UPR 8521, Tecnosud, Rambla de la thermodynamique, 66100 Perpignan, France;
email : francoise.massines@ promes.cnrs.fr ; Tel. : (+33) 04 68 68 27 03
[+] *Jean-François Lelièvre now at Photovoltaic Module Laboratory (LMPV), National Institute for Solar Energy (INES-CEA), 50, avenue du Lac Léman, 73375 Le Bourget du Lac, France*

ABSTRACT

This work demonstrates the efficient optical and passivation properties provided by hydrogenated silicon nitride (SiN_x:H) layers deposited in a lab-scale atmospheric pressure (AP) PECVD reactor, meeting all requirements for the in-line realization of high efficiency PERC solar cells. Good thickness and optical constant homogeneities were achieved by applying modulated low frequency plasma (200 kHz). The use of voltage amplitude modulation enabled discharge optimization and led to greatly enhanced SiN_x film homogeneity and conformity. Low effective reflectivity R_{eff} = 2.8% was consequently achieved on alkaline textured surface. Additionally, AP-PECVD SiN_x showed good thermal stability and low absorption coefficient, demonstrating that such layers could act as efficient antireflective coatings. Besides, outstanding surface passivation properties were obtained after firing, both on n-type FZ c-Si substrates of standard doping (τ_{eff} = 1.45 ms) and on highly doped n^+ emitters (j_{0e} = 74±2 fA.cm^{-2}). Finally, AP-PECVD SiN_x thin films were tested on industrial PERC-type

solar cell architectures, which demonstrated the potential of applying these layers both as efficient rear-side capping layer and front-side antireflective coating. The first PERC solar cell results featuring AP-PECVD SiN_x layers pave the way for upscaling the Dielectric Barrier Discharge lab-scale reactor in an industrial in-line process able to provide low cost and high throughput SiN_x capping and antireflective layers.

Keywords: Hydrogenated silicon nitride SiN_x:H, Atmospheric Pressure PECVD, PERC solar cells, passivation layer, antireflective coating.

INTRODUCTION

The crystalline silicon-based photovoltaic industry is rapidly moving towards the Passivated Emitter and Rear Cell (PERC) structure[1,2,3,4,5], which allows conversion efficiencies well above 21% and is forecasted to become the dominant solar cell technology within next few years[6]. Thus, developing high efficiency (> 21%) PERC solar cells while simultaneously reducing their fabrication costs is of major interest for the photovoltaic community. In particular, significant cost reduction can be achieved by developing alternative processes in order to minimize wafer handling and avoid vacuum processes. For instance, PERC solar cells currently require three vacuum-based processes for the deposition of the passivation layers: hydrogenated silicon nitride SiN_x:H antireflective coating (ARC) on the front side and AlO_x/SiN_x passivation stack layers on the rear side[3,4]. Aluminum oxide (AlO_x) providing high quality rear passivation properties can already be deposited at atmospheric pressure by using high throughput spatial Atomic Layer Deposition (ALD)[7] technique. However, a technological bottleneck for increasing the solar cell production throughput is the deposition of SiN_x thin layers at atmospheric pressure conditions. Indeed, such a process would be compatible with a fully in-line fabrication process and would avoid the need for expensive vacuum equipment.

The innovative deposition tool explored in this work is based on direct Atmospheric Pressure Plasma Enhanced Chemical Vapor Deposition (AP-PECVD) using a homogeneous dielectric barrier discharge (DBD)[8,9,10] in $Ar/SiH_4/NH_3$ gas mixture. As the plasma density is much higher at atmospheric pressure (AP – 10^{11}-10^{13} cm^{-3}) than at low pressure (LP – 10^{8}-10^{10} cm^{-3}), the challenge is to maintain a stable plasma at AP in order to obtain dense and homogeneous SiN_x films on large surfaces. To date, homogeneous, powder-free SiO_x or SiN_x layers have been obtained on small surfaces by AP-PECVD in different reactor configurations, however, the corresponding optical and passivation properties still needed improvement for photovoltaic applications[11,12]. For instance, a drawback of PECVD at atmospheric pressure is that the mean free path of radicals in the plasma is very small (< 1 µm) compared to deposition at low pressure. This factor can explain the lack of coating conformity observed on textured silicon surfaces, i.e. the SiN_x film is thicker on the top than on the bottom of the pyramid[13]. In order to reach the objective of process industrialization, AP-PECVD SiN_x layers must demonstrate optimum optical and passivation properties[14,15]. Thus, we have studied in detail AP-PECVD SiN_x optical properties as well as passivation properties on lowly and highly doped Si surfaces in order to apply the optimum results in realizing high efficiency PERC solar cells. The results presented here show that AP-PECVD in a configuration close to industrial corona reactors, thus

fully compatible with industrialization[8,11], can lead to SiN_x thin films suitable for high efficiency low cost PERC solar cells.

EXPERIMENTAL

a) AP-PECVD reactor and SiN_x deposition process optimization

Figure 1-a shows a schematic view of the lab-scale AP-PECVD reactor developed at PROMES: the gases are injected between the dielectric square bars, reaching two plasma zones (surface S = 15×50 mm^2; gap = 1 mm) where film deposition occurs. The two plasma zones are defined by the high voltage (HV) electrodes, that is, the electrical metallization of the lower inner face of the 3mm-thick dielectric alumina bars (Al_2O_3). In order to maintain the plasma during substrate displacement, the grounded lower electrode surface is much larger than the upper electrode and is separated from the plasma zone by another 3mm-thick alumina plate. Such Dielectric Barrier Discharge (DBD) configuration allows controlling the high voltage discharge along the 1 mm-height gas gap, minimizing the current increase and thus avoiding the transition from low temperature plasma to arc discharge. The gas mixture is composed of ammonia (NH_3) and silane (SiH_4) as reactive gases, and argon (Ar) as dilution gas, with a fixed argon gas flow of 3 slm and a constant sum of the reactive gas flows (SiH_4 + NH_3) equal to 200 ppm. The use of Ar as dilution gas allows decreasing drastically the plasma voltage breakdown, Ar-NH_3 being a Penning mixture[8]. For plasma frequency higher than 50 kHz, such conditions allow to avoid arc micro-discharges and to obtain a stable glow discharge[16]. Depending on the applied voltage and frequency, the ammonia-to-silane gas flow ratio R = NH_3/SiH_4 was adjusted in order to obtain the adequate SiN_x stoichiometry for antireflection purpose (refractive index n = 2 for non-encapsulated solar cells[17]). In addition, the incorporation of deflectors at the plasma exit (see Figure 1-a) allowed to greatly avoid the gas recirculation, which is correlated to Si powder formation and thus incorporation in the SiN_x layer. Such modification of the DBD deposition head design led to a strong decrease of the light absorption (extinction coefficient k) within AP-PECVD SiN_x thin films[12]. An interesting feature of this AP-PECVD lab-scale reactor is that the discharge mode can be adjusted over a wide range of frequencies (50 kHz – 7.3 MHz), providing a unique tool for the study of the influence of such plasma sources on the final SiN_x optical and passivation properties[13]. However, currently the Si wafer size that can be processed in such a small reactor is limited to ½ solar cell size (156×78 mm^2), on which homogeneous and dense SiN_x layer can be obtained on a maximum surface of 45×55 mm^2 through sample holder displacement (Figure 1-b). This is nonetheless adequate for the fabrication of

40×40 mm^2 lab-scale PERC solar cells using industrial-size solar cell processing tools, which can provide representative results for process optimization and validation.

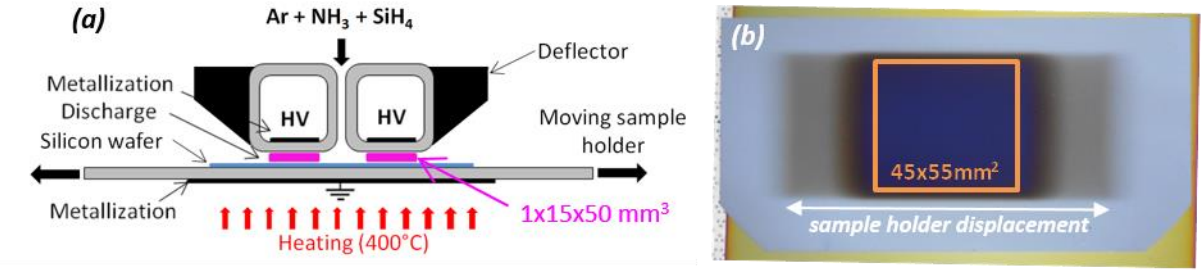

Figure 1 : (a) Schematic view of the AP-PECVD discharge cell. (b) ½ cell-size Si wafer (156×78 mm^2) coated by AP-PECVD SiN_x with homogeneous properties on a maximum surface of 45×55 mm^2.

Unless stated, all the AP-PECVD deposition processes were performed at 400°C applying a modulated low frequency plasma of around 200 kHz, which is the limit between Glow and Townsend discharge modes characterized by current amplitude diminution[8]. Such excitation frequency was found to lead to the best surface passivation results in previous works[12]. The use of amplitude modulation (see Figure 2-a), defined by modulation frequency f_m and duty cycle $DC = t_{on}/(t_{on}+t_{off})$, allows optimizing the discharge mode by finding the balance between radical dissociation (plasma on) and surface reaction (plasma off). Indeed, the applied modulation was found to greatly enhance SiN_x film homogeneity and conformity thanks to a better distributed radical dissociation along the plasma zone[18], i.e. avoiding total consumption of reactive gases during the corresponding gas residence time (fixed at 30 ms through fixed gap and Ar gas flow). Figure 2-b shows the measured voltage and current as a function of time when the plasma was on (during t_{on}), and at four distinct times during SiN_x deposition (t = 0; 5'; 10' and 15'). It clearly demonstrates the extreme stability of the discharge during deposition.

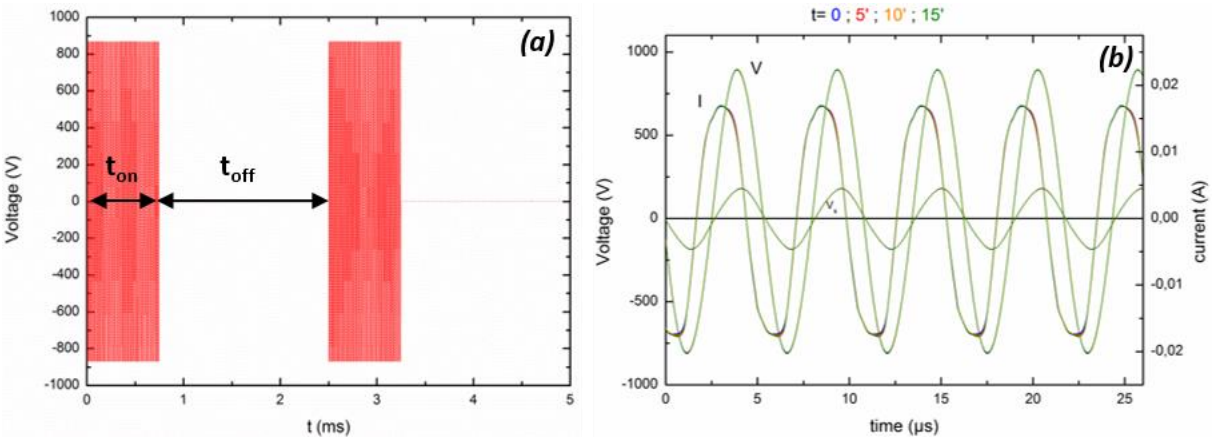

Figure 2: (a) Example of applied voltage amplitude modulation with f_m=400Hz and DC=$t_{on}/(t_{on}+t_{off})$=30%; (b) Applied Voltage (V) and measured Current (I) as a function of time for a 184 kHz discharge (during t_{on}). The measurements were performed at four distinct times during SiN_x deposition (0, 5', 10', 15').

Preliminary experiments were performed to determine the adequate plasma modulation parameters for discharge optimization. Figure 3 shows the picture of a textured ½ cell-size wafer used for process optimization in the static mode, i.e. without sample holder movement. Three different static-mode AP-PECVD SiN_x layers were deposited at three different spots of the Si wafer and the deposited areas correspond approximately to the size of the two plasma zones (15×50mm^2), as illustrated by the picture of the DBD deposition head. When no modulation was applied (plasma always on – Figure 3-b), the deposited SiN_x coating had an inhomogeneous thickness along each 15 mm-wide plasma zone and high concentration Si powder incorporation was clearly identified by powder light diffusion. Due to reactor configuration (see Figure 1-a), the gas residence time in the plasma is rather long (30 ms) and significant variations of the plasma chemistry are expected along the direction of the gas flow. Thus, when no modulation was applied, the plasma was always on with a high power density P of 1.2W.cm^{-3}. In this case, the reactive gases are believed to be fully consumed in the beginning of the plasma zone. Furthermore, the high power plasma is believed to promote Si powder formation and incorporation in the SiN_x layer. The application of plasma modulation led to greatly improved SiN_x layer homogeneity. The different graphs of Figure 3 show the schematic shapes of the applied modulated voltage according to modulation frequency (f_m=33, 66, 100, 200 Hz – DC=30%) and compared to the 30 ms residence time of the gas in each plasma zone. The total power density is defined by P_{tot}=P×DC, where P is the full applied power during the time t_{on} for which the plasma is on. For the modulation parameters studied here, the total power was the same for all cases (P_{tot}=0.36 W.cm^{-3}), but the consecutive absolute on- and off-times (t_{on}+t_{off}) were strongly decreased with increasing frequency. Through DC, discharge

modulation induced the reduction of the total discharge power P_{tot} and thus the energy for a given gas residence time (or position along the plasma zone). As the dissociation mechanism of silane only depends on the plasma energy density "seen" by SiH_4 since it enters the plasma, the dissociation of silane is negligible during the off-time t_{off}, which allows increasing the radical diffusion process and facilitates surface reaction[18]. Increasing time for radical transport (t_{off}) is thus believed to lead to an improvement of SiN_x coating homogeneity and density.

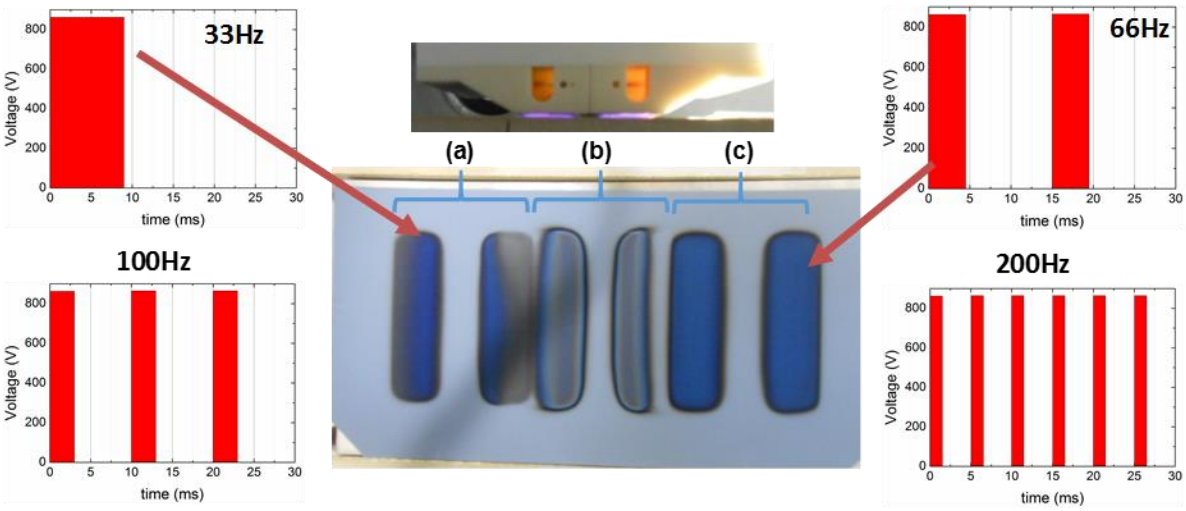

Figure 3 : Pictures of DBD deposition head and of textured ½ cell-size wafer with three static-mode AP-PECVD SiN layers deposited under the two 15×50mm² plasma zones (R=NH_3/SiH_4=2; f≈184kHz; DC=30%; t=7') and varying the modulation frequency: (a) f_m=33Hz; (b) no modulation; (c) f_m=66Hz. The graphs show the schematic shapes of the applied modulated voltage according to f_m (DC=30%) compared to the 30ms residence time of the gas molecules in each plasma zone (400 Hz not shown).

Indeed, homogeneous SiN_x layers were obtained in the static mode over the whole plasma zone surface for $f_m \geq 66$ Hz (DC = 30%) as illustrated by Figure 3-c. The deposited SiN_x surface and color were the same for higher f_m (100, 200 and 400 Hz, not shown here), indicating identical stable plasma reactions and deposition velocity (constant P_{tot}). In this case, the reactive gases were not totally consumed along the plasma zone. On the other hand, for a modulation frequency of 33 Hz, the on-time (t_{on} = 9 ms) appeared to be too long, leading to complete dissociation of the reactive gases before they reached the plasma exit and consequently to inhomogeneous SiN_x layers (Figure 3-a). A similar study was realized according to DC for a constant f_m = 100Hz, showing homogeneous plasma deposition for DC ϵ [20-50%]. DC greater than 60% led to inhomogeneous SiN_x layers caused by Si clusters formation and incorporation associated with a complete dissociation of the reactive gases before they reached the plasma

exit. Therefore, the corresponding t_{on} = 6 ms appears to be the upper limit for stable plasma deposition. In the dynamic mode, i.e. moving the sample holder backward and forward, the experiments were thus performed varying the modulation frequency f_m between 66 Hz and 400 Hz and the duty cycle DC between 20% and 50%.

b) Si sample preparation and thin film characterization

For surface passivation and ellipsometry studies, 4-inches FZ n-type and p-type Si wafers (280 µm thick; 2.8Ω.cm; DSP) were HF cleaned before SiN_x deposition by AP-PECVD, varying plasma parameters. The limited size of the lab-scale reactor implied using truncated 4-inches Si wafers (height limited to 80 mm) on which homogeneous SiN_x could be deposited on a surface of 45×55 mm^2 (see Figure 8-b). The thickness *w*, wavelength-dependent refractive index $n(\lambda)$ and extinction coefficient $k(\lambda)$ of the different SiN_x films were deduced by spectroscopic ellipsometry (Horiba UVISEL), applying Tauc–Lorenz dispersion model[19]. The average minority charge carrier effective lifetime was measured in the center of the wafer using QSSPC technique[20] (Sinton WCT-120 tool) for an injection level of $\Delta n=10^{15}$ cm^{-3}. Under the assumption that FZ c-Si samples have equally high bulk charge carrier lifetime (τ_b), the extracted values of the effective lifetime (τ_{eff}) can be used as a measure of the surface passivation quality of the different SiN_x layers[15]. The effective lifetime was systematically measured before and after rapid thermal annealing at around 820°C for a duration of 1 s (JetFirst RTA furnace – SEMCO Technologies). The goal of such RTA process was to improve SiN_x surface passivation properties while simulating the co-firing of solar cell contacts (usually performed in an industrial IR-lamp belt furnace). The QSSPC measurement technique was also used to determine the emitter saturation current density j_{0e} which is directly related to the emitter passivation quality. The obtained j_{0e} values were systematically corrected using Kimmerle j_0 analysis method[21]. Besides, charge carrier effective lifetime mappings were recorded using both microwave photoconductance decay (µW-PCD – Semilab WC-2000) and lifetime calibrated photoluminescence (PL) imaging[22]. It was decided to use Si wafers passivated on the rear side by standard Low Pressure (LP) PECVD SiN_x layers in order to avoid rear side contamination from the (not so clean) environment of the reactor when opening it at 200°C. The reference samples with LP-PECVD SiN_x deposited on both sides exhibited a high effective lifetime after RTA (τ_{eff} ~ 1.5 ms), corresponding to a surface recombination velocity (SRV) lower than 10 $cm.s^{-1}$. In this way, the AP-PECVD SiN_x layer deposited on the front side controls predominantly the measured lifetime as it is supposed to lead to a lower quality surface passivation. This hypothesis is valid until SRV provided by AP-PECVD SiN_x reaches values

obtained with LP-PECVD SiN_x (~10 $cm.s^{-1}$). Therefore, lifetime measurements performed on such pre-passivated Si wafers gave an upper limit of SRV provided by AP-PECVD SiN_x layers. In addition, SiN_x film conformity studies were performed on magnetically casted Czochralski-grown (MCz) p-type Si wafers cut in ½ cell-size using an IR laser (1060 nm). Such wafers were previously cleaned and alkaline textured at Fraunhofer ISE. The thin film conformity was deduced from reflectivity measurements[13] using an integrating sphere (Labsphere).

c) *Passivation samples (j_{0e} ; iV_{oc}) and PERC solar cell fabrication processes*

Apart from AP-PECVD processes performed at PROMES, ½ cell-size samples used for passivation studies (j_{0e} ; iV_{oc}) and PERC solar cells were entirely fabricated at the PV-TEC pilot line of Fraunhofer ISE in a close-to-industrial manner[23]. All samples were processed together following the shared fabrication flow described in Figure 4, with some variations according to the targeted characterization technique.

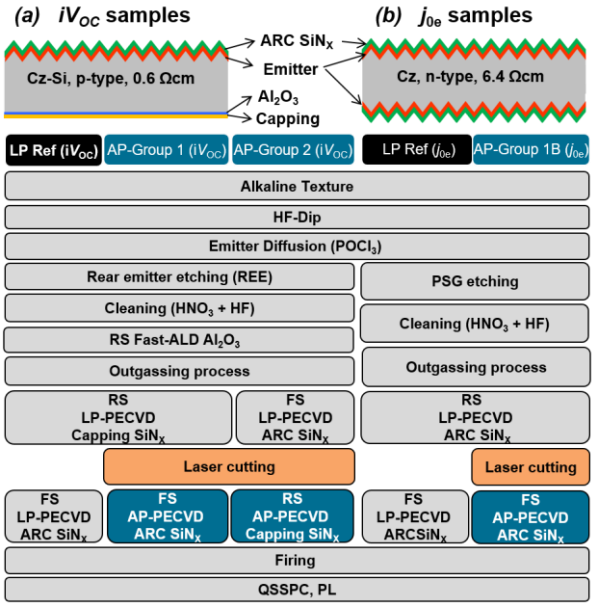

Figure 4: Schematic final structure and process flow used for the fabrication of (a) iV_{oc} and (b) j_{0e} samples. FS and RS respectively represent the front and the rear-sides of the sample.

The starting material was pseudo-square 156×156 mm^2 MCz p-type Si wafers with an initial wafer thickness of 180 µm and specific base resistivity of 0.6 Ω.cm. First, saw-damage removal was performed in an alkaline solution, followed by alkaline texturing process in a batch wet-chemical bench, leading to a resulting wafer thickness of 160 µm. Then, the textured wafers underwent emitter diffusion process in a tube diffusion furnace using $POCl_3$ as precursor gas. The diffusion process was adjusted to form n^+ emitters with sheet resistance values (R_{SH}) close

to 85 Ω/sq. No emitter window was applied so that the complete wafer surface was diffused. Afterwards, rear-side emitter removal process was performed and the surfaces were cleaned by hot HNO_3 solution followed by HF-Dip and DI water rinsing. For iV_{oc} samples and PERC solar cells, a 6 nm-thick Al_2O_3 layer was then deposited on the rear-side by using ultrafast spatial atomic layer deposition (ALD) process[7]. This step was followed by the so-called outgassing process, which is a 10 minutes low temperature annealing under N_2 at 550°C performed mainly to avoid blistering of the rear-side stack layer[4]. Next, the wafers were distributed into 3 different groups for the deposition of SiN_x antireflection coating (ARC) and/or capping layer on the front and rear sides, respectively, by using either LP-PECVD or AP-PECVD deposition techniques. The reference group samples were processed on both sides by LP-PECVD (150 nm capping layer then 75 nm ARC). Meanwhile, some samples were cut in half using an IR laser (1060 nm) in order to proceed to AP-PECVD SiN_x deposition at PROMES. These samples were distributed in two groups: Group 1 (75 nm LP-PECVD SiN_x ARC / laser cut / 100 nm AP-PECVD SiN_x capping layer) and Group 2 (150 nm LP-PECVD SiN_x capping layer / laser cut / 75 nm AP-PECVD SiN_x ARC). It was preliminary verified that no HF cleaning was needed before SiN_x deposition on both sides, simplifying greatly the fabrication process.

For iV_{oc} experimental protocol (see Figure 4-a), the samples were then fired in an IR-lamp belt furnace at a peak temperature of 820°C. Thus, these wafers underwent all the fabrication steps of PERC solar cells except the metallization process. Such asymmetrical samples were used to extract the implied open-circuit voltage iV_{oc} at 1 sun illumination by QSSPC measurements[20], giving reliable information of the surface passivation level that is achievable on solar cell architectures. Simultaneously, Group 1B was processed as emitter dark saturation current density (j_{0e}) measurement samples by depositing SiN_x on symmetrically textured and diffused samples. Starting from MCz 6.4 Ω.cm n-type Si wafers, the process flow was the same as described before, except that the rear emitter etching was substituted by phosphorus glass etching while AlO_x layer was not deposited on the rear side (see Figure 4-b). Instead, these samples were coated on the rear side by LP-PECVD ARC, then laser cut in half before they were sent to PROMES for AP-PECVD ARC deposition. The j_{0e} samples were finally sent back to Fraunhofer ISE where they underwent the in-line belt-firing process before QSSPC and PL measurements. For PERC solar cells, the process flow was the same as iV_{oc} samples until front and rear passivation layers (see Figure 4-a). The rear-side stack was then opened using the IR laser, and screen-printing was applied to metallize both front and rear sides of the wafers using Ag and Al pastes, respectively. Since the AP-PECVD depositions were performed on a small

surface of the wafer (45×55 mm^2), a special front side Ag-grid featuring 1 busbar (0.8 mm width) and 28 fingers (35 ± 3 µm width) was designed to form solar cells of 40×40 mm^2 area. Finally, the PERC solar cells were fired in an in-line IR-lamp belt furnace before I-V characterization.

RESULTS

a) Optical properties

Spectroscopic ellipsometry measurements were performed on 10 different points along the central 45×55mm^2 homogeneous SiN_x surface and showed good thickness *w* and refractive index *n* homogeneities ($\Delta w \leq 2$ nm; $\Delta n \leq 0.02$). Furthermore, the AP-PECVD SiN_x layers demonstrated good stability upon annealing (Rapid Thermal Annealing at 820°C during 1s), showing a slight film densification, the thickness being reduced by 1nm and the refractive index being stable or slightly decreased ($\Delta n \leq -0.02$). The same behavior was observed on control reference samples coated by low pressure (LP) PECVD SiN_x. The deposition velocity *v* was found to be independent of the gas flow ratio $R=NH_3/SiH_4$ whereas it was slowed down on textured wafers. However, the major parameter that controls the deposition velocity is the total discharge power ($P_{tot}=P\times DC$). For a fixed applied power P (i.e. the full applied power during the time t_{on} for which the plasma is on – see Figure 2-a), *v* depends linearly on the duty cycle $DC = t_{on}/(t_{on}+t_{off})$: for instance, *v* increases from 4 $nm.min^{-1}$ to 10 $nm.min^{-1}$ for 200 kHz glow discharge when DC increases from 20% to 50%. On the other hand, the refractive index *n*, which is directly related to the SiN_x composition and density, depends on $R=NH_3/SiH_4$ as well as on P_{tot} and P.

For non-encapsulated lab solar cells, the optimum antireflective coating (ARC) refractive index *n* should be equal to 2 for a central wavelength of λ = 600 nm, associated with a film thickness of *w* = 75 nm[17]. These parameters are easily obtained adjusting the gas flow ratio $R=NH_3/SiH_4$ but as described in previous works[12], the absorption within the AP-PECVD SiN_x layer was at first much higher than LP-PECVD standard ARC. Great effort has been dedicated to reduce to negligible values the correlated extinction coefficient *k*, with for instance, the application of deflectors in the new DBD deposition head, reducing Si cluster incorporation in the layer, as already described. For encapsulated solar cells (n_0=1.45), the optimum refractive index should be equal to 2.39 (λ = 600 nm) combined with a thickness of *w* = 63 nm [17]. However, increasing the SiN_x refractive index is correlated to the increase of the extinction coefficient and thus

absorption within the thin film. Generally, a compromise is found with a moderately high SiN_x refractive index showing very little absorption ($n \approx 2.1$ – w = 71 nm).

With the objective of further reducing the light absorption within the AP-PECVD SiN_x antireflective coating, thus increasing the photogenerated current in the final solar cell, an experiment was launched to evaluate the effect of the plasma modulation on SiN_x optical properties. As already highlighted, a balance between radical dissociation (plasma on) and surface reaction (plasma off) should be found. DC was varied from 20% to 50%, the other parameters being fixed (f = 184 kHz ; P= 1 $W.cm^{-3}$; f_m = 400 Hz ; R = NH_3/SiH_4 = 1.74). Figure 5 shows the corresponding AP-PECVD SiN_x refractive index *n* and extinction coefficient *k* measured by spectroscopic ellipsometry. Reference LP-PECVD SiN_x optical constants are also shown for comparison for two distinct stoichiometries (*n* = 1.97 and *n* = 2.1 at λ = 600 nm, respectively).

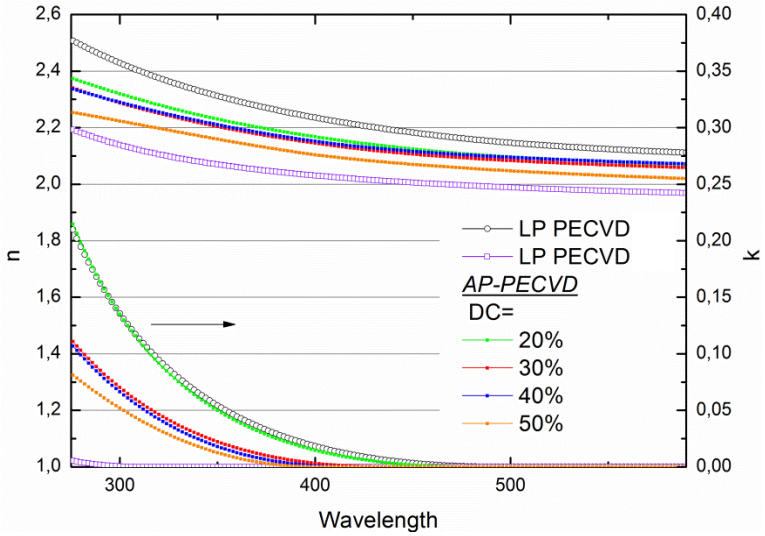

Figure 5 : Wavelength-dependent refractive index n(λ) and extinction coefficient k(λ) of different AP-PECVD SiN_x layers obtained with different duty cycles DC (f = 184 kHz ; P= 1 $W.cm^{-3}$; f_m = 400 Hz ; R = NH_3/SiH_4 = 1.74). Reference LP-PECVD SiN optical constants are shown for comparison.

The total discharge power (P_{tot}=P×DC) increased with the duty cycle, leading to an increase of the deposition velocity. However, the refractive index *n* stayed rather constant for DC∈[20% ; 50%], indicating a stable plasma reactivity. The increase in power for DC = 50% may have induced a more efficient NH_3 dissociation and thus a denser N-richer SiN_x layer, with a slight decrease of *n* (and *k*). On the other hand, it can be observed that the AP-PECVD SiN_x layers exhibited very low extinction coefficient, comparable to LP-PECVD SiN_x films. Interestingly, these results show that, for a similar refractive index, the extinction coefficient can be minimized modifying the duty cycle, *k* being reduced from 0.2 (DC = 20%) to 0.08 (DC = 50%)

at λ = 240 nm. For DC = 20%, Si powder may have been incorporated in the SiN_x layer during the corresponding longer t_{off}, leading to stronger absorption (Si-Si bonds). However, the Si cluster incorporation is believed to keep the resulting refractive index low because of lower film density. For higher DC, the absorption was reduced for a similar refractive index, indicating both diminution of Si-Si bonds and film densification. Consequently, for a modulation frequency of f_m = 400 Hz, the optimum DC appeared to be between 30% and 50% in order to obtain dense powder-free and low absorption SiN_x layers. Another experiment was carried out in parallel, varying the modulation frequency f_m (33-400 Hz) and keeping the duty cycle constant (DC=30%), the other parameters being fixed: f = 184 kHz; P = 1.2 $W.cm^{-3}$; $R = NH_3/SiH_4 = 2$. Thus, the total discharge power was the same for all the samples (P_{tot}= P×DC = 0.36 $W.cm^{-3}$) associated with a constant deposition velocity (v=7 $nm.min^{-1}$). Increasing f_m led to a negligible increase of the optical constants *n* and *k*. Consequently, optimal SiN_x optical properties were obtained for f_m between 100 Hz and 200 Hz, for which both plasma reaction stability and low SiN_x absorption ($k \leq 0.08$ at 240 nm) were obtained.

The SiN_x film conformity on textured wafers was improved since our last published results, with an effective reflectivity R_{eff} (which takes into account the wavelength dependent solar spectrum irradiance[17]) lowered from 3.5% to 2.9% [12,13]. However, the modulation parameters (f_m; DC) were not found to further improve film conformity. This phenomenon is illustrated in Figure 6-a which shows the reflectivity measurements performed on alkaline textured Si wafers coated by either LP-PECVD reference SiN_x layer or AP-PECVD SiN_x layers obtained at low frequency (LF – 184 kHz) or at radio frequency (RF – 5.3 MHz, see below). Whereas LP-PECVD reference layer (R_{eff} = 2.5%) shows a zeroed reflectivity at the central wavelength (λ = 600 nm) due to destructive interferences through adequate *n* and *w*, the AP-PECVD films lead to a minimum reflectivity at the central wavelength that is not fully zeroed (R_{eff} = 2.9%). Indeed, the lack of film conformity, i.e. the gradual thickness variation of the SiN_x coating along the pyramids, leads to a combination of distinct reflectivity curves averaged at the macroscopic scale, consistent with the obtained reflectivity curve[13]. Another solution to improve film conformity could be to apply a modulated radio frequency voltage excitation (RF > 1 MHz) to create the plasma. In such high frequency discharge, ions (and powder) are confined in the plasma and a high power discharge can be easily obtained, leading to high deposition velocity. After plasma parameters optimization, the selected modulated frequency (5.3 MHz; V_{cc} = 672 V; f_m = 100 Hz; DC=30%) led to homogeneous SiN_x films on acidic and alkaline textured Si wafers over the maximum surface allowed by our lab-scale reactor (45×55 mm^2),

which is to our knowledge the first time such homogeneous RF SiN_x layers are deposited at atmospheric pressure. The RF films showed a slightly improved film conformity compared to LF (R_{eff} = 2.8% - see Figure 6). As we finally manage RF AP-PECVD SiN_x deposition, the next step will be to apply tailored voltage waveforms (TVW) combining high-energy RF discharge for radical dissociation during t_{on} and LF voltage on the counter electrode during t_{off}. The latter should help to increase the mean free path of radicals in the plasma thus improving surface reactions and film conformity[24].

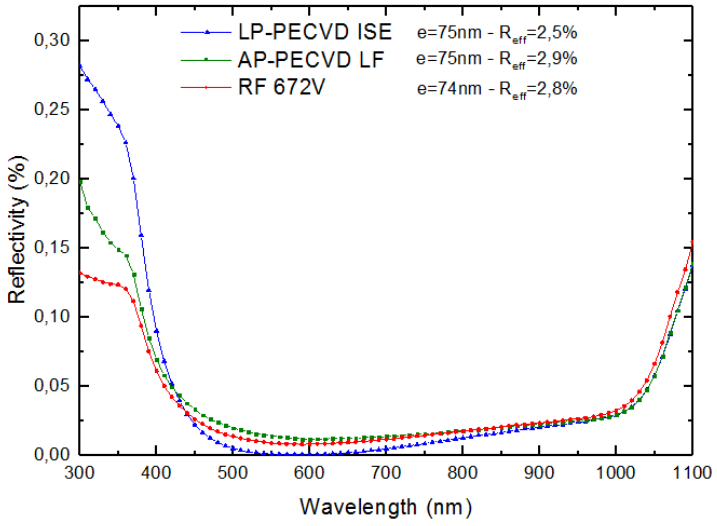

Figure 6: Reflectivity measurement of reference ARC SiN_x layer deposited by LP-PECVD compared to AP-PECVD ARC layers deposited at low frequency (184Hz) and radiofrequency (5.3 MHz). Film thickness and corresponding effective reflectivity are also indicated.

Nevertheless, reasonably low effective reflectivity values were obtained with AP-PECVD films, and the side effect inducing lower reflectivity for short wavelengths when compared to conformal layers (see Figure 6) may partly compensate the optical losses at intermediate wavelengths, especially for high efficiency well passivated PERC solar cells.

b) Surface passivation properties

Additionally to act as good ARC for Si solar cells, AP-PECVD SiN_x layers must demonstrate high quality surface passivation properties, on the one hand, to provide efficient emitter passivation on the front surface and, on the other hand, to effectively cap the 6nm-thick AlO_x rear passivation layer. Experiments were carried out to evaluate the effect of plasma modulation parameters on SiN_x surface passivation properties. First, the modulation frequency was fixed (f_m =400 Hz) and the duty cycle was varied (20% < DC < 50%), the other parameters being fixed: f = 184 kHz; P = 1 $W.cm^{-3}$; R = NH_3/SiH_4 = 1.74. The SiN_x deposition time was adjusted

to obtain similar film thicknesses (≈ 75 nm). Indeed, he total discharge power (P_{tot}=P×DC) increases with the duty cycle, leading to an increase of the deposition velocity. Figure 7-a shows the measured minority charge carrier effective lifetime τ_{eff} according to DC before and after firing FZ n-type Si substrates (ρ=2.8 Ω.cm) coated with SiN_x (LP-PECVD on the rear side, as already described). The as-deposited SiN_x layers provided a moderate surface passivation quality with lifetime values ranging from 45 µs to 113 µs. After RTA, lifetime increased strongly in all cases with an outstanding value of 1062 µs for DC=30%, corresponding to a surface recombination velocity SRV < 15 cm.s^{-1}. An optimum was found around DC = 30% (DC = 40% offers reasonable good surface passivation as well). This observation may be related to an optimum film density, as indicated previously through ellipsometry measurements.

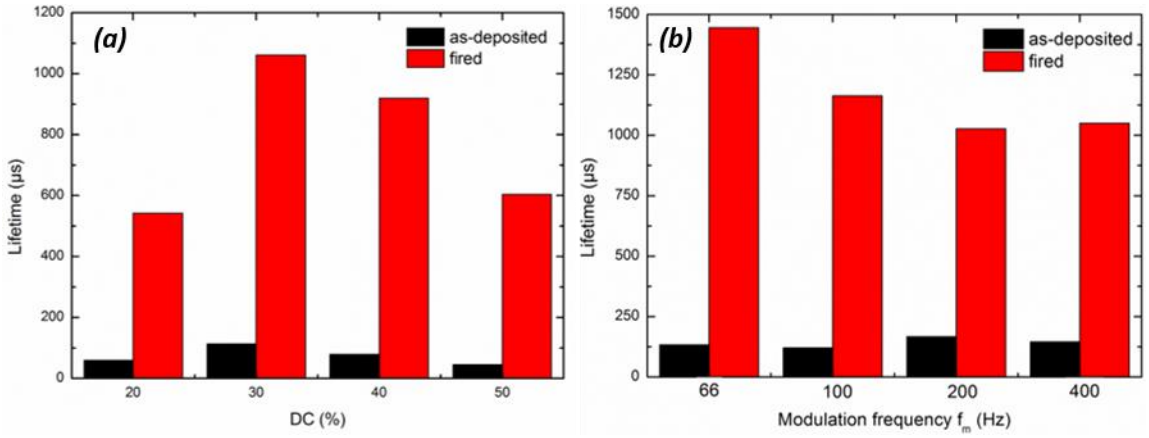

Figure 7: Minority charge carrier effective lifetime τ_{eff} before and after RTA ($\Delta n=10^{15}$ cm^{-3}) according to plasma (a) modulation duty cycle DC (f=184kHz; P=1W.cm^{-3}; f_m=400Hz; R=NH_3/SiH_4=1.74) and (b) modulation frequency f_m (f=184kHz; P=1.2W.cm^{-3}; DC=30%; R=2).

Figure 7-b shows τ_{eff} according to modulation frequency f_m, before and after firing (f = 184 kHz; P = 1.2 W.cm^{-3}; DC = 30%; R = NH_3/SiH_4 = 2). As-deposited samples exhibited moderately good surface passivation properties, the lifetime values ranging from 104µs to 166 µs. The results were slightly improved in comparison with the DC experiment, which could be attributed to a higher and better-controlled plasma power (P= 1.2 W.cm^{-3}). After RTA, lifetime increased strongly in all cases with final values higher than 1 ms. For f_m= 66 Hz, an outstanding value of 1.45ms was obtained, corresponding to SRV < 10 cm.s^{-1}. For such high lifetimes, the front AP-PECVD SiN_x layer may no longer be the limiting measurement factor, as surface passivation quality becomes similar to LP-PECVD SiN_x films applied on the rear side. Nevertheless, for all cases, such measurement method provides an upper limit of SRV and the

obtained values are very close to LP-PECVD SiN_x layers whatever the modulation frequency. Parallel experiments were performed on FZ p-type Si leading to similar tendencies. As expected for p-type material, the measured SRV were higher than for n-type Si[14,15]. The lowest values (SRV < 40 $cm.s^{-1}$, comparable to reference LP-PECVD SiN_x) were obtained applying modulation parameters (f_m; DC) either equal to (66 Hz; 30%) or (100 Hz; 40%).

Furthermore, effective lifetime mappings (see Figure 8) demonstrated a very homogeneous lifetime distribution along the SiN_x layer, independently of the film thickness. Indeed, similar and even higher lifetimes were measured outside of the central uniform surface, where only one of the two plasma zones passed completely over the Si surface, thus leading to SiN_x thickness *w* of less than 40 nm (see pictures Figure 8-b and Figure 1-b). This confirms that surface passivation provided by SiN_x becomes efficient for small thicknesses, at least lower than 40 nm. At the extreme edges of the wafer, the lifetime was degraded over ~1cm, probably due to surface discontinuity at the edges of the Si wafer causing filamentary arc discharge development.

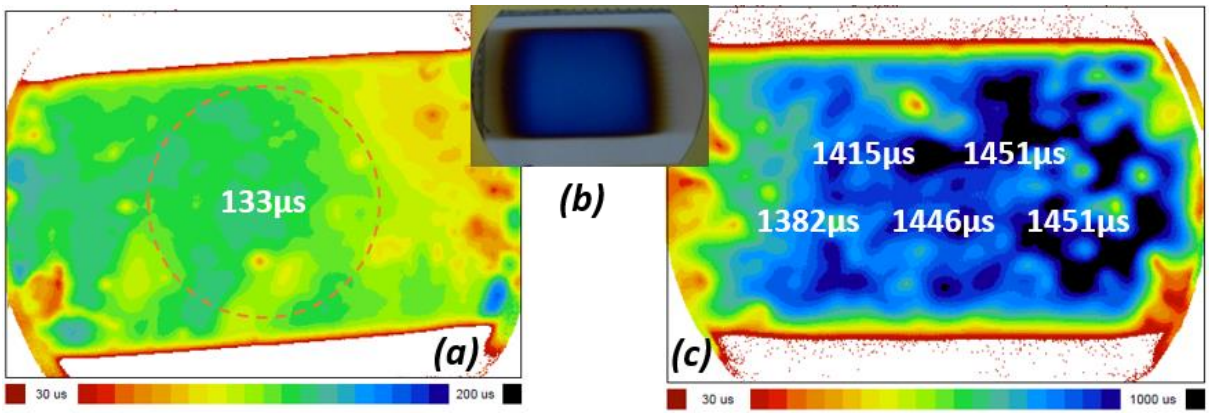

Figure 8 : µW-PCD minority charge carrier effective lifetime τ_{eff} mappings (a) before and (c) after RTA of a Si substrate (4'' n-type FZ, 2.8 Ω.cm) passivated on the front side by AP-PECVD SiN_x (f=184kHz; P=1.2W.cm^{-3}; f_m=66Hz; DC=30%; R=NH_3/SiH_4=2). On the maps are indicated the average Sinton PCD τ_{eff} at $\Delta n=10^{15}$ cm^{-3} measured on different spots of the Si wafer (circle = size of Ø40mm sensor). (b) Picture of a truncated 4'' n-type Si wafer coated with AP-PECVD SiN_x layer.

c) Front emitter passivation, rear capping layer and PERC solar cells

A cross test experimental protocol was launched with the goal of applying the optimized AP passivation layers (according to f, f_m, DC, P...) to industrial-like diffused and textured ½ cell-size wafers (see experimental details). In this work plan, the front side ARC and the rear side AlO_x/SiN_x passivation stack layer were tested independently and jointly on asymmetrically processed wafers, which underwent all the PERC solar cell fabrication steps, except

metallization. On such asymmetrical samples, the implied open-circuit voltage (iV_{oc}) at 1 sun illumination obtained from PCD-lifetime measurements gives reliable information of the surface passivation level on solar cell architectures. According to plasma stability, optical and passivation properties, the selected optimized AP-PECVD plasma power and modulation parameters were: f = 185 kHz; V_{cc} = 1.76 kV; P = 1.2 W.cm^{-3}; f_m = 100 Hz; DC = 40%; R = 2.

Firstly, Group 1 was used to provide insights into the application of AP-PECVD SiN_x (w = 75 nm) as front ARC and passivation layer on PERC-type architectures with rear side capped by LP-PECVD SiN_x. Simultaneously Group 1B was prepared as emitter dark saturation current density (j_{0e}) measurement samples by depositing SiN_x on symmetrically textured and diffused samples, with the rear surface passivated by LP-PECVD SiN_x. On the other hand, Group 2 allowed testing of the rear side capping of AlO_x by AP-PECVD SiN_x (w = 100 nm) on PERC-type architectures where the front ARC SiN_x layer was deposited by LP-PECVD. In addition, the reference group samples were prepared by applying both front and rear SiN_x depositions by using LP-PECVD process. Figure 9-a shows the iV_{oc} values obtained before and after firing for the different groups of samples.

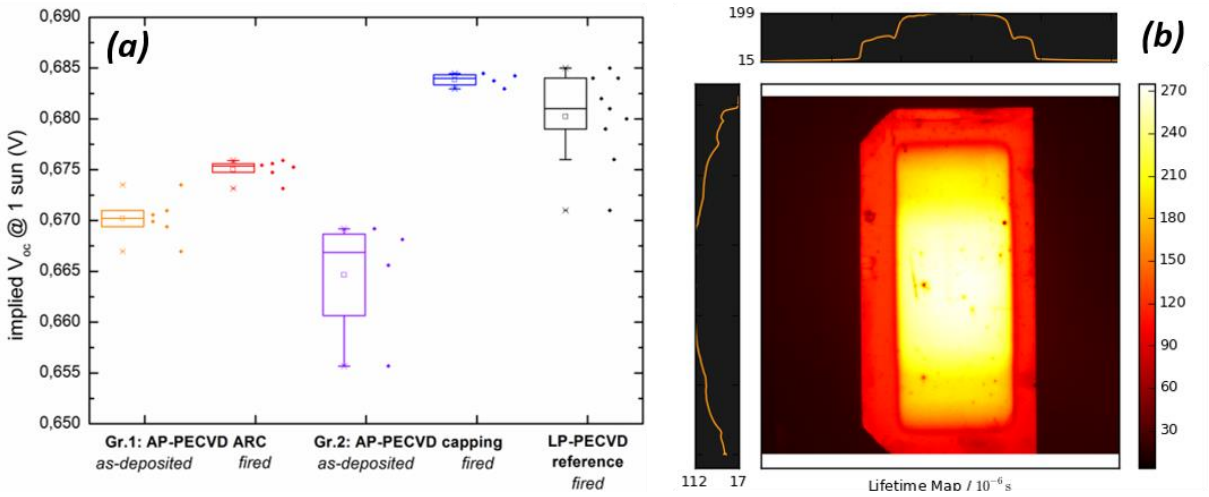

Figure 9: (a) Implied V_{oc} at 1 sun, before and after firing, for the different groups of samples used to evaluate AP-PECVD SiN_x as front ARC layer or rear capping layer (f=185kHz; P=1.2W.cm^{-3}; f_m=100Hz; DC=40%; R=2). (b) PL mapping of a sample from Group 1B (j_{0e}).

The firing step in an industrial IR lamp belt furnace strongly improved surface passivation quality, especially in the case of AP-PECVD SiN_x capping layer (group 2), with final iV_{oc} tightly distributed around a mean value of 684 mV. Such values were among the highest iV_{oc} obtained with reference LP-PECVD samples in this batch, showing the good potential of AP-

PECVD SiN_x to act as capping layer. Group 1 wafers also showed a tight iV_{oc} distribution after firing with a mean value of 675 mV. Although iV_{oc} were lower in this case, the emitter surface passivation provided by AP-PECVD SiN_x can still be considered as reasonably good to compete with LP-PECVD due to their lower production cost to the latter. Indeed, the as-deposited emitter dark saturation current density j_{0e} measured on group 1B samples reached a low mean value of 97±3 fA.cm^{-2}, which was greatly improved to 74±2 fA.cm^{-2} after firing and is close to the values obtained by LP-PECVD reference group (j_{0e}=52±1 fA.cm^{-2}). Furthermore, lifetime and photoluminescence (PL) mappings demonstrated homogeneous SiN_x surface passivation properties in the intended central region area (45×55 mm^2) of the samples (see Figure 9-b). In this case, the mappings showed clearly a better lifetime in the central homogeneous surface (white region in PL mapping) in comparison to the edge of the sample with thinner layer (yellow region) where only one plasma zone "saw" the Si wafer (see corresponding picture Figure 1-b). This observation indicates that for highly doped surfaces such as emitters, thicker and/or more homogeneous SiN_x layers lead to a better surface defect passivation, possibly due to more efficient hydrogenation during firing. These results suggest that AP-PECVD SiN_x layers can provide efficient emitter passivation properties. This statement was confirmed in the next step by the realization of the first PERC-type solar cells featuring AP-PECVD SiN_x layers.

The illuminated current–voltage measurement results are summarized in Table 1 for the very first PERC solar cells that could be fabricated. As it will be discussed later on, these preliminary results were obtained on few cells because of the high breakage rate of our work plan (½ cell-size wafers). Furthermore, the current–voltage measurements were performed on ½ cell-size wafers without cutting the cell off. A black cardboard mask with an opening of 40x40 mm² was placed on the wafer during the measurement, and the rear electrode was contacted by a copper plate. It is important to note that the measurement was not calibrated and that the reference cell used did not have the same size or the same metallization design. Consequently, the current values measured and the resulting efficiency should be considered as a comparison with the LP reference process and not as an absolute value. Nevertheless, as illustrated by j_{sc} and V_{oc} distribution (Figure 10), these results confirm the previously established tendency in a consistent way.

Table 1: Illuminated current–voltage parameters of PERC solar cells fabricated to evaluate AP-PECVD SiN_x layers as front ARC (Group 1) or rear capping layer (Group 2): energy conversion efficiency η, fill factor FF, short-circuit current density j_{SC} and open-circuit voltage V_{OC}.

Group (Front/rear passivation)		η (%)	FF (%)	j_{sc} (mA.cm^{-2})	V_{oc} (mV)
Group 1	*Best cell*	19.9	78.4	39.1	649
(AP/LP)	***Average 4 cells***	**19.5 ± 0.3**	**78.2 ± 0.5**	**38.9 ± 0.2**	**641 ± 7**
Group 2	*Best cell*	20.6	79.1	39.3	661
(LP/AP)	***Average 2 cells***	**20.4 ± 0.2**	**78.7 ± 0.3**	**39.3 ± 0.06**	**659 ± 2**
Reference	*Best cell*	20.5	78.6	39.7	656
(LP/LP)	***Average 13 cells***	**20.2 ± 0.2**	**78.4 ± 0.6**	**39.4 ± 0.2**	**654 ± 2**

First, the best cell was obtained with AP-PECVD SiN_x capping layer (20.6% - Group 2), demonstrating that such coating can already be applied as industrial rear side capping layer. Indeed, the associated relatively high V_{oc} (mean value of 659 mV) indicates an improved surface passivation at the rear side when applying AP-PECVD SiN_x, which may be related to a better hydrogenation of the surface during firing and/or a longer time at 400°C during SiN_x deposition (eventually improving AlO_x activation). The other parameters (*FF*, j_{sc}) stayed similar to reference LP-PECVD solar cells, as could be expected.

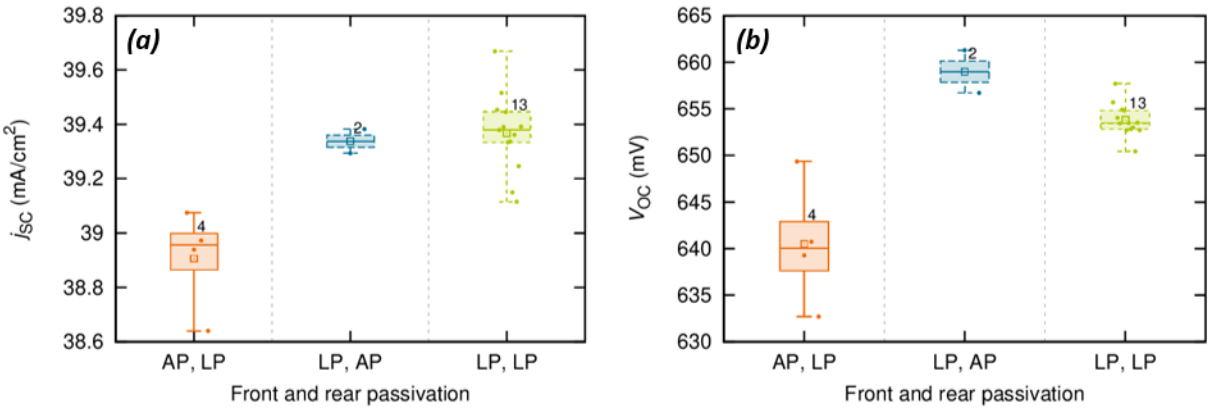

Figure 10: Distribution of (a) short-circuit current density j_{SC} and (b) open-circuit voltage V_{OC} measured on 40×40 mm^2 PERC solar cells fabricated using LP-PECVD SiN_x as front and rear layers (reference group LP,LP) and AP-PECVD SiN_x as front ARC layer (Group 1 – AP,LP) or rear capping layer (Group 2 – LP,AP), the opposite layer being deposited by LP-PECVD.

When AP-PECVD SiN_x films were used as front ARC and passivation layer, the average efficiency decreased to 19.5% due to a reduction of both j_{sc} and V_{oc}, as could be expected. On one hand, the higher effective reflectivity R_{eff} due to a lack of film conformity (see Optical

properties) is directly related to the photogenerated current and thus to j_{sc}. On the other hand, iV_{oc} and j_{0e} measurements showed that AP-PECVD SiN_x films exhibit adequate but less effective emitter passivation properties when compared to standard LP-PECVD. This is confirmed by the obtained V_{oc} = 641 mV, associated with a large standard deviation that might be related to a deposition process with a higher sensitivity on surface chemical cleaning. Nevertheless, the best PERC cell led to a conversion efficiency η = 19.9%, very close to our initial goal of 20%. As discussed in the following, the design and fabrication of a pre-industrialization AP-PECVD reactor prototype could avoid the drawbacks of the lab-scale reactor, leading to enhanced film properties. Thus, AP-PECVD SiN_x layers remain promising candidates for front and rear passivation of high efficiency low cost PERC solar cells.

DISCUSSION

The baseline PERC solar cell process realized at Fraunhofer ISE with industrial-scale equipment was reaching typically an iV_{oc} of 680-685 mV corresponding to final efficiency of 21.0% when applied on 6-inch pseudo-square wafers[3,4]. The cell fabrication process was adapted to ½ cell-size wafers in order to apply AP-PECVD, leading to a cell area of 40×40 mm^2 without emitter windows. As far as the reference group is concerned, the process adaptations were probably responsible for the difference between the expected efficiency (21.0%) and the measured efficiency (20.2%). The main difference with 6-inch PERC solar cells is the average fill factor FF = 78.4% (similar for all groups), which is 2% lower than the expected results[4]. Such difference in FF is probably mainly due to the metallization process and the presence of a large emitter area remaining in the dark (under the mask) during the I-V measurements. Nonetheless, the experimental protocol implied sample transport, handling, storage and processing during long periods (up to several months before SiN_x deposition) demonstrating the long-standing stability of both AlO_x 6 nm-thick layers at the rear surface as well as the protective layer obtained at the front side during the outgazing process. Furthermore, control wafers were added to the experimental samples in order to evaluate the transport/handling impact on the results: ½ cell-size wafers were *(i)* processed at ISE following all the fabrication steps of iV_{oc} samples until and including the rear capping layer deposited by LP-PECVD; *(ii)* then transported to PROMES; *(iii)* then put in another box and stored; *(iv)* then back to ISE; *(v)* then processed at ISE applying the last fabrication steps, i.e. front side ARC by LP-PECVD followed by firing and characterization (see Figure 4). These control wafers showed similar iV_{oc} results (included in Figure 9-a) and similar dispersion as LP-PECVD reference samples entirely processed at ISE. Additionally, a PERC solar cell was processed with one of those samples

(included in Figure 10), leading to one of the highest efficiencies (20.4%), clearly demonstrating the weak impact of wafer transportation and handling on the results.

In this context, PERC solar cells with AP-PECVD SiN_x as capping layer reached the expectancy of good protective (and hydrogenation?) layer, leading to similar and even better results than reference LP-PECVD PERC solar cells. On the other hand, AP-PECVD SiN_x led to lower efficiencies when applied as ARC, essentially due to *(i)* a lack of film conformity (reducing light transmission to the cell and thus j_{sc}) and *(ii)* less efficient emitter passivation properties than LP-PECVD SiN_x layers (thus decreasing V_{oc}). Indeed, the correlated emitter saturation current density was higher for AP-PECVD SiN_x layers (j_{0e} = 74 ± 2 fA.cm^{-2}) than for LP-PECVD films (j_{0e} = 52 ± 1 fA.cm^{-2}). Nevertheless, such j_{0e} value is relatively low if compared to state-of-the-art published values[2-5], which demonstrates competitive SiN_x emitter passivation properties while having still some room for its improvement through AP plasma optimization. For instance, the development of RF discharges modulated through tailored voltage waveform (TVW) may lead to better film conformity and passivation properties.

Looking at these first results, it can be highlighted that AP-PECVD groups comprised limited number of samples (e.g. only 3 for Group 1B, however with a tight dispersion). Indeed, we had a high wafer breakage rate during the transnational experimental protocol due to various parameters such as transportation, handling and processing of ½ cell-size Si wafers with small thickness (w = 160µm). For instance, such wafer size could be problematic for the industrial-size equipment of ISE, such as screen printing metallization or co-firing belt furnace, which are designed for full-sized cells. Consequently, part of the samples were lost (2-3 of each group, initially composed of 10 wafers). On the other hand, AP-PECVD SiN_x deposition processes on ½ cell-size wafers were frustrated for a long time because of Si wafer bending and sliding, leading eventually to wafer breakage. We demonstrated that this phenomenon was due to inhomogeneous temperature at the edges of the sample holder (see Figure 1-a), inducing a strong temperature gradient within the thin Si wafer, thus causing wafer bending. Although we finally fixed this problem, many of the samples were broken, mechanically damaged and/or led to bad layer homogeneity and composition when bending occurred during AP-PECVD SiN_x deposition. Indeed, wafer bending induced the reduction of the gap between the upper electrode and the Si wafer, allowing the generation of arc micro-discharges that are detrimental to thin film deposition. Therefore, the further improvement of AP-PECVD SiN_x optical and passivation properties appeared to be limited by the size of the laboratory prototype reactor developed at PROMES. Actually, the advantages of such a small reactor are numerous (e.g.

controlled atmosphere, adjustable gap, ideal for plasma study, wide range of DBD discharge modes...). However, some drawbacks were identified as affecting both the experiments and the final SiN_x properties: *(i)* the sample size that can be processed is limited (½ cell-size Si wafers - 156×78 mm^2); *(ii)* the deposition process is time-consuming due to heating and cooling times (in contrast with fast IR lamp belt furnaces); *(iii)* the temperature is not homogeneous at the edges of the chuck (which induces wafer bending for thin wafers); *(iv)* and the sample holder has to be displaced backward and forward in the dynamic mode (in contrast with a continuously moving belt furnace). Such sample holder displacement is believed to induce the incorporation within SiN_x layers of detrimental Si powder formed at the exit of the plasma zones and brought back in the plasma reactive volume during the "trip back" of the chuck[12]. In this context, upscaling the AP-PECVD reactor would allow to eliminate all these drawbacks, consequently improving SiN_x deposition process, and thus final SiN_x properties. Accordingly, the work presented here brings strong arguments to design and develop a semi-industrial scale reactor comprising multiple deposition heads in a belt furnace configuration, with the objective of realizing high efficiency low cost PERC solar cells.

CONCLUSION

For the first time, atmospheric pressure PECVD process was successfully applied for the realization of high efficiency PERC solar cells. We demonstrated that the complex challenge of depositing uniform and dense SiN_x layers by plasma at atmospheric pressure could be tackled by optimizing the discharge mode and finding the balance between radical dissociation and surface reaction. The direct correlation between plasma modulation parameters and the optical and passivating properties of AP-PECVD SiN_x thin films was studied in detail. Accordingly, the best SiN_x optical and passivation performance was obtained applying a modulated 200 kHz Glow Dielectric Barrier Discharge, using a modulated frequency of f_m = 100 Hz and a duty cycle of DC = 40%. Such SiN_x coatings were successfully integrated in PERC structures demonstrating efficient properties both as rear side capping layer and as front side antireflective and passivation layer. Furthermore, it was highlighted that the lab-scale AP-PECVD reactor configuration may limit the further improvement of SiN_x optical and passivation properties. However, the drawbacks of this prototype, such as temperature inhomogeneity, maximum Si wafer size or Si cluster formation and incorporation in the SiN_x layer, could be avoided through the design and development of a semi-industrial scale reactor. The combination of optimized reactor configuration for thin film deposition at atmospheric pressure and the application of new discharge modulation modes such as radio frequency tailored voltage waveforms (TVW)

offers promising perspectives for the realization of fully in-line low cost and high efficiency PERC solar cells.

ACKNOWLEDGEMENTS

The authors would like to thank the French Environment and Energy Management Agency (ADEME) for financing this research within the project APPI under the contract number 1505C000A. The federal ministry for economic affairs and energy (BMWi) of Germany is also acknowledged for funding the German part of APPI project under the contract number 0325895A. The authors give thanks to Frederic Cortés Juan and Guillermo Sanchez from Universitat Politècnica de València (Spain) for complementary ellispometry measurements.

REFERENCES

[1] Blakers AW, Wang A, Milne AM, Zhao J, and Green MA. 22.8% efficient silicon solar cell. Appl. Phys. Lett. 1989; 55:13; 1363–1365.

[2] Min B, Wagner H, Müller M, Neuhaus H, Brendel R, Altermatt P.P. Incremental efficiency improvements of mass-produced PERC cells up to 24%, predicted solely with continuous development of existing technologies and wafer materials. Proc. 31st Eur. Photovolt. Sol. Energy Conf. Exhib., Hamburg, Germany, pp. 473–476 (Sept 2015).

[3] Werner S, Lohmüller E, Saint-Cast P, Greulich JM, Weber J, Schmidt S, Moldovan A, Brand AA, Dannenberg T, Mack S, Wasmer S, Demant M, Linse M, Ackermann R, Wolf A, Preu R. Key aspects for fabrication of p-type Cz-Si PERC solar cells exceeding 22% conversion efficiency. Proc. 33rd Eur. Photovolt. Sol. Energy Conf. Exhib., Amsterdam, The Netherlands, (Sept. 2017).

[4] Saint-Cast P, Werner S, Greulich J, Jager U, Lohmuller E, Hoffler H, Preu R. Analysis of the losses of industrial-type PERC solar cells. Phys. Status Solidi A 2016; 1-7.

[5] Dullweber T, Hannebauer H, Dorn S, Schimanke S, Merkle A, Hampe C, and Brendel R. Emitter saturation current densities of 22 fA/cm^2 applied to industrial PERC solar cells approaching 22% conversion efficiency. Prog. Photovolt: Res. Appl. 2017; 25: 509–514.

[6] International Technology Roadmap for Photovoltaic ITRPV, 9th edition, March 2018.

[7] Lien S-Y, Yang C-H, Wu K-C, and Kung C-Y. Investigation on the passivated Si/Al_2O_3 interface fabricated by non-vacuum spatial atomic layer deposition system. Nanoscale Res. Lett. 2015; 10:93.

[8] Massines F, Sarra-Bournet C, Fanelli F, Naude N and Gherardi N. Atmospheric Pressure Low Temperature Direct Plasma Technology: Status and Challenges for Thin Film Deposition. Plasma Process Polym 2012; 9: 1041-1073.

[9] Starostin SA, Premkumar PA, Creatore M, Veldhuizen EM, Vries H, Paffen RMJ, Sanden MCM. On the formation mechanisms of the diffuse atmospheric pressure dielectric barrier discharge in CVD processes of thin silica-like films. Plasma Sources Sci. Technol. 2009; 18(4): 045021.

[10] Belmonte T, Henrion G, Gries T. Nonequilibrium Atmospheric Plasma Deposition. J. Therm. Spray. Tech. 2011; 20: 744.

[11] Kakiuchi H, Ohmi H and Yasutake K. Atmospheric-pressure low-temperature plasma processes for thin film deposition. J. Vac. Sci. Technol. A 2014; 32: 030801.

[12] Massines F, Silva J, Lelièvre J-F, Bazinette R, Vallade J, Lecouvreur P, Pouliquen S. Hydrogenated Silicon Nitride SiN_x:H Deposited by Dielectric Barrier Discharge for Photovoltaics. Plasma Process. Polym. 2016; 13:1; 170-183.

[13] Bazinette R, Lelièvre J-F, Gaudy L, Massines M. Influence of the Discharge Mode on the Optical and Passivation Properties of SiN_x:H Deposited by PECVD at Atmospheric Pressure. Energy Procedia 2016; 92:309-316.

[14] Cuevas A, Kerr MJ, Schmidt J. Passivation of crystalline silicon using silicon nitride. WCPEC-3, Osaka, Japan, (May 2003).

[15] Lelièvre J-F, Fourmond E, Kaminski A, Palais O, Ballutaud D and Lemiti M. Study of the composition of hydrogenated silicon nitride SiN_x:H for efficient surface and bulk passivation of silicon. Sol. Energy Mater Sol. Cells 2009; 93: 1281.

[16] Bazinette R, Subileau R, Paillol J, Massines F. Identification of the different diffuse dielectric barrier discharges obtained from 50kHz to 9MHz in Ar/NH_3 at atmospheric pressure. Plasma Sources Sci. Technol. 2014 ; 23: 035008.

[17] Honsberg C, Bowden S. Photovoltaics: Devices, Systems and Applications (PVCDROM). Sydney: University of New South Wales; 1998. pveducation.org; last visit 20/06/18.

[18] Vallade J, Bazinette R, Gaudy L and Massines F. Effect of glow DBD modulation on gas and thin film chemical composition: Case of $Ar/SiH_4/NH_3$ mixture. J Phys D Appl Phys. 2014; 47(22): 224006

[19] Jellison GE, Modine FA. Parameterization of the optical functions of amorphous materials in the interband region. Appl. Phys. Lett. 1996; 69:3; 371–373; erratum: 69:14; 2137 (1996).

[20] Sinton RA, Cuevas A. Contactless determination of current–voltage characteristics and minority-carrier lifetimes in semiconductors from quasi-steady-state photoconductance data. Appl. Phys. Lett. 1996; 69:17; 2510–2512.

[21] Kimmerle A, Greulich J, Wolf A. Carrier diffusion corrected J_0-analysis of charge carrier lifetime measurements for increased consistency. Sol. Energy Mater. Sol. Cells 2015; 142: 116–122.

[22] Giesecke JA, Schubert MC, Schindler F and Warta W. Harmonically Modulated Luminescence: Bridging Gaps in Carrier Lifetime Metrology Across the PV Processing Chain. IEEE J. Photovolt. 2015; 5:1; 313-319.

[23] Biro D, Preu R, Glunz SW, Rein S, Rentsch J, Emanuel G, Brucker I, Faasch T, Faller C, Willeke G, and Luther J. PV-TEC: Photovoltaic technology evaluation center - design and implementation of a production research unit. Proc. 21st Eur. Photovolt. Sol. Energy Conf. Exhib., Dresden, Germany, pp. 621–624 (2006).

[24] Brunet P, Rincon R, Matouk Z, Chaker M and Massines F. Tailored waveform of Dielectric Barrier Discharge to monitor composite thin film morphology. Langmuir 2018; 34:5; 1865–1872.